

Journal of Materials Chemistry A

Accepted Manuscript



This is an *Accepted Manuscript*, which has been through the Royal Society of Chemistry peer review process and has been accepted for publication.

Accepted Manuscripts are published online shortly after acceptance, before technical editing, formatting and proof reading. Using this free service, authors can make their results available to the community, in citable form, before we publish the edited article. We will replace this *Accepted Manuscript* with the edited and formatted *Advance Article* as soon as it is available.

You can find more information about *Accepted Manuscripts* in the [Information for Authors](#).

Please note that technical editing may introduce minor changes to the text and/or graphics, which may alter content. The journal's standard [Terms & Conditions](#) and the [Ethical guidelines](#) still apply. In no event shall the Royal Society of Chemistry be held responsible for any errors or omissions in this *Accepted Manuscript* or any consequences arising from the use of any information it contains.

COMMUNICATION

Lead acetate precursor based p-i-n perovskite solar cells with enhanced reproducibility and low hysteresis

Cite this: DOI: 10.1039/x0xx00000x

Dávid Forgács, Michele Sessolo and Henk J. Bolink*

Received 00th January 2012,
Accepted 00th January 2012

DOI: 10.1039/x0xx00000x

www.rsc.org/

A low temperature approach for the fabrication of p-i-n perovskite solar cells is presented. Using lead acetate-based precursors, flat and homogeneous $\text{CH}_3\text{NH}_3\text{PbI}_3$ films, compatible with the use of thin organic charge transport layers, can be obtained. The correspondent solar cells showed power conversion efficiency up to 12.5%, with remarkable reproducibility and very low hysteresis.

Photovoltaic devices employing organic-inorganic (hybrid) halide perovskites as the active layer have become a major field of research since the pioneering work of Miyasaka and his co-workers.¹ In few years, the power conversion efficiencies (PCE) of the devices increased from 3.8% to the current record of 20.1 %², approaching the performance of mature technologies such as silicon solar cells, and solidifying its place as a possible disruptive technology in the market. Hybrid perovskites possess desired properties for application in photovoltaics, such as high absorption coefficient, wide range of absorption in the visible part of the solar spectrum, direct band gap³, long carrier diffusion lengths⁴ and the possibility to be produced by solution processing, potentially leading to cheap, large scale, roll-to-roll compatible fabrication. Despite the high reported efficiencies, there are still several issues that need to be addressed before this technology is ready for mass production. One key objective is to develop more reliable and consistent deposition processes.^{5, 6} It is well understood that the crystalline structure of the perovskite plays a crucial role in the device characteristics.^{7, 8} Therefore, to successfully achieve reproducible high performance solar cells, the perovskite crystallization process needs to be controlled either by proper choice of processing parameters, techniques⁹ and/or by material selection. For high performance diodes, smooth, trap- and pinhole-free layers with large crystal sizes¹⁰ are desired to allow for thick active layers with good transport properties.¹¹ Within this

perspective, different preparation methods have been developed. The perovskite active layer can be deposited by vacuum processing, either by co-¹²⁻¹⁴, sequential-¹⁵, or flash evaporation¹⁶, and by solution processing from a precursor solution¹⁷ or a sequential deposition¹⁸ method. In the latter approach, various solvents have been used – i.e. dimethylformamide (DMF)¹⁹ dimethylsulfoxide (DMSO)²⁰, or *N*-methyl-2-pyrrolidone (NMP).¹⁰ Initially, lead iodide and methylammonium iodide had been used to prepare the pure iodide perovskite material, $\text{CH}_3\text{NH}_3\text{PbI}_3$. Soon after, it was demonstrated that by replacing lead iodide with lead chloride, devices with better performances could be obtained.²¹ This has been referred to as the mixed halide route, even though the amount of chloride in the final perovskite is negligible.²² It has been shown that the spectating ion has an effect on the crystal growth kinetics and that, by exchanging the iodide with other anions, the properties of the resulting perovskite layer could be significantly altered. Moore et al. compared the crystallization pathways of perovskites obtained from several lead precursors (iodide, chloride, acetate and nitrate) by monitoring the material growth with in situ wide-angle X-ray scattering.²³ They have found particularly favourable kinetics when using the lead acetate precursor, i.e. long processing windows for the obtainment of large crystalline perovskite domains at low temperature. This route has been applied in several approaches to explore the possibilities it provides to prepare optoelectronic and photovoltaic devices.²⁴⁻²⁶ The highest performance from the latter group is reported by Zhang et al., who prepared perovskite solar cells with the lead acetate precursor and obtained smooth, pinhole-free perovskite films, resulting in devices with a champion PCE of 15.2%.²⁷ They have used an n-i-p (“standard”) device configuration, where the perovskite was deposited onto a compact TiO_2 layer. Such architecture requires a high temperature annealing treatment, and as such it cannot be directly implemented on plastic foils, or in multi-

junction devices. Moreover, those solar cells show a pronounced hysteresis during the J-V characterisation, making the extraction of the key device parameters somewhat ambiguous. The origin of hysteresis in perovskite solar cells is still under investigation, however it has been shown to be extremely sensitive on the characterization conditions (scan speed, pre-bias, temperature, etc.).²⁸ Perovskite p-i-n planar heterojunctions have been demonstrated to show less-pronounced hysteretic behaviour, in virtue of a more electronically favourable electron extraction interface.^{29, 30} With these premises, we have applied the lead acetate precursor route to the fabrication of p-i-n solar cells employing organic semiconductors as charge transport layers. These devices can be prepared at low temperature and are thus more compatible with roll-to-roll fabrication³¹. Here we show that the perovskite layers fabricated by a one-step deposition method from a lead acetate precursor lead to reproducible and efficient p-i-n solar cells with negligible hysteretic J-V behaviour.

Device preparation

Methylammonium iodide (MAI) was purchased from Lumtec, lead acetate trihydrate ($\text{Pb}(\text{OAc})_2$) was purchased from Aldrich, and both materials were used as received. The substances were mixed in a nitrogen filled glovebox to yield a 40 wt% solution in anhydrous DMF with a 3 to 1 molar ratio of MAI to $\text{Pb}(\text{OAc})_2$, and stirred overnight. Glass substrates with an indium-doped tin-oxide (ITO) coating were subsequently cleaned in a detergent solution, Millipore water, and isopropyl alcohol, then transferred to a UV-ozone chamber for 20 minutes of treatment. Afterwards, an 80 nm thick poly(3,4-ethylenedioxythiophene) doped with poly(styrenesulfonate) (PEDOT:PSS, Clevis PVP AI 4083 from Hereaus) film was deposited in air, and annealed at 130 °C for 15 minutes. The substrates were then transferred to a N_2 -filled glovebox. The perovskite precursor solution was filtered and spin-coated on top and the resulting layers were annealed at 90 °C on a hot plate. The perovskite formation was monitored by recording the UV-Vis spectrum every 5 minutes. A layer of phenyl-C61-butiric acid methyl ester (PCBM) was then deposited from a 2 wt% chlorobenzene solution, and the metal contacts (10 nm Ba capped with 80 nm Ag) were thermally evaporated on top. Device characterization was performed using a mini-sun simulator with a halogen lamp designed by ECN and calibrated with a Si reference cell. The unencapsulated solar cells were measured in a N_2 -filled glovebox. The current density (J) versus voltage (V) characteristics were collected in the dark and under illumination using a shadow mask to prohibit lateral current collection from outside the active area.

Results and Discussion

The evolution of the pristine precursor layers was followed by an optical absorption measurement, monitoring the band-edge transition of the $\text{CH}_3\text{NH}_3\text{PbI}_3$ perovskite. Interestingly, the typical strong, broad absorption centered between 750 and 775 nm was already observed after only 5 minutes annealing at 90 °C (Fig. 1a), in accordance with the favourable formation kinetics of the perovskite

from the lead acetate precursor. Longer annealing resulted in only a slight increase of the absorption at the bandgap energy, and after 20 minutes no change could be observed, suggesting the quantitative conversion of the precursor compound to $\text{CH}_3\text{NH}_3\text{PbI}_3$. The crystallinity of the perovskite was investigated by grazing incidence X-ray diffraction (GIXRD) measurements, revealing the pattern (in terms of both peak position and relative intensity²⁰) of a typical pure-iodide perovskite (Fig. 1b). One sample was continuously measured in air and, after approximately 10 hours, the diffraction peak of lead iodide appeared and started to grow (see Supplementary Information), indicating the decomposition of the perovskite due to the presence of oxygen and moisture.

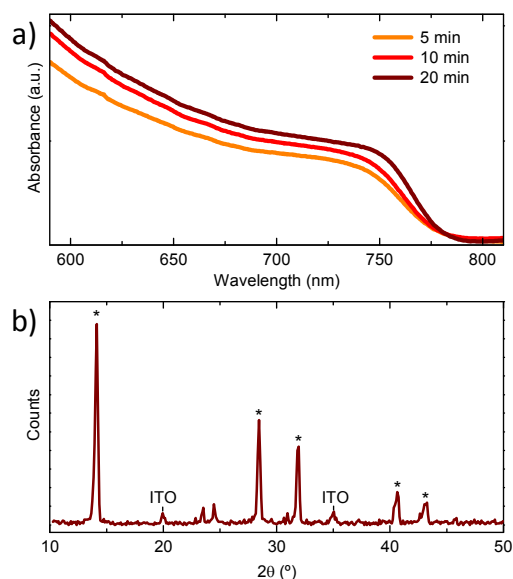


Fig. 1. UV-Vis absorption (a) of a perovskite thin film with increasing annealing time at 90 °C. GIXRD spectra (b) of the thin film after annealing for 20 minutes. The characteristic diffraction peaks as well as those arising from the ITO substrate are highlighted.

The $\text{CH}_3\text{NH}_3\text{PbI}_3$ perovskite layers were further characterized by atomic force microscopy (AFM) and scanning electron microscopy (SEM), in order to investigate their surface morphology and structure. The AFM topography (Fig. 2a) revealed a homogeneous surface composed of closely packed, fine grains.

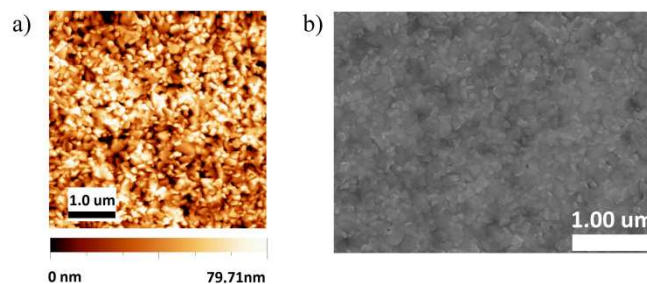


Fig. 2. AFM topography (a) and SEM (b) image of the perovskite surface deposited on ITO/PEDOT:PSS.

The correspondent root mean squared roughness, calculated over an area of $25 \mu\text{m}^2$, was found to be 19.05 nm. This indicates a very smooth surface, and allows the use of thin organic selective layers to sufficiently cover the perovskite material and prevent surface recombination at the top metal contact. The SEM analysis (Fig. 2b) confirms the homogeneous and pinhole-free film morphology, with grain sizes of approximately 100 nm in diameter. Perovskite solar cells, with the structure ITO/PEDOT:PSS/ $\text{CH}_3\text{NH}_3\text{PbI}_3$ /PCBM/Ba-Ag, were fabricated following the previously described method. The J-V curves were recorded between -0.2 and 1.2V with 0.01V steps, integrating the signal for 20 ms after a 20 ms delay. This corresponds to a speed of 250 mV/s which is similar to that used by Zhang et al. in their work, allowing a direct comparison between their n-i-p and our p-i-n architecture.²⁷ We have extended the range to even lower scan speeds, where the hysteresis becomes even smaller (see Fig. S2 in the Supporting Information). Generally, pixels on the same substrate (area of 9cm^2) have very similar performances, independently on the position. This fact highlights the potential of this deposition route for large-area solution processing of perovskite cells. To stress the homogeneity of the layers, the J-V curves corresponding to four pixels (0.0264 cm^2) on the same substrate are reported in Fig. 3a, and the correspondent figures of merit shown in Table 1. The open circuit voltage V_{oc} varies in the range of 950-960 mV, which is slightly lower compared to what is commonly observed in high efficiency perovskite solar cells, but in agreement with a previous work using the same lead precursor.²⁷

Table 1. Device parameters from the J-V curves depicted on Fig. 3a.

Forward scan			
V_{oc} (mV)	J_{sc} (mA/cm^2)	FF (%)	PCE (%)
960	18.2	67.4	11.8
953	18.1	65.5	11.3
958	18.9	66.0	11.9
956	18.8	69.0	12.4
Reverse scan			
V_{oc} (mV)	J_{sc} (mA/cm^2)	FF (%)	PCE (%)
963	18.2	67.6	11.8
953	18.1	66.4	11.5
957	18.9	66.9	12.1
954	18.8	69.7	12.5

The recorded short circuit current density J_{sc} and FF values are 18-19 mA/cm^2 and 65-70%, respectively. The champion device prepared with this approach exhibited a PCE of 12.5%. The thickness of the active layer measured with a mechanical profilometer was approximately 300 nm. Such thickness enables high light harvesting and allows the charges to leave the active layer before recombining, as demonstrated by the high external quantum efficiency (EQE, inset of Fig. 3a). Thicker layers would increase the absorption and charge generation, so that devices with higher photocurrents could be realized. However, we have observed a decrease in the fill factor and hence in the device performance for perovskite layer thicknesses exceeding 300 nm. This is most likely due to the morphology of the active layer, which is composed by fine grains approximately 100 nm in size. While these dimensions result in a flat and homogeneous film surface, they might hinder an efficient extraction of charges from thick active layers.¹⁰ During the I-V measurements, virtually no hysteresis was observed between the curves recorded in forward (negative to positive) and reverse (positive to negative) bias. J_{sc} and V_{oc} shows less than 1 % difference between the forward and reverse scans in all measured devices. The FF is in general slightly higher in the reverse scan, in agreement with most reports on hybrid perovskite solar cells, and it is independent on precursor material or processing method.^{27, 29, 32}

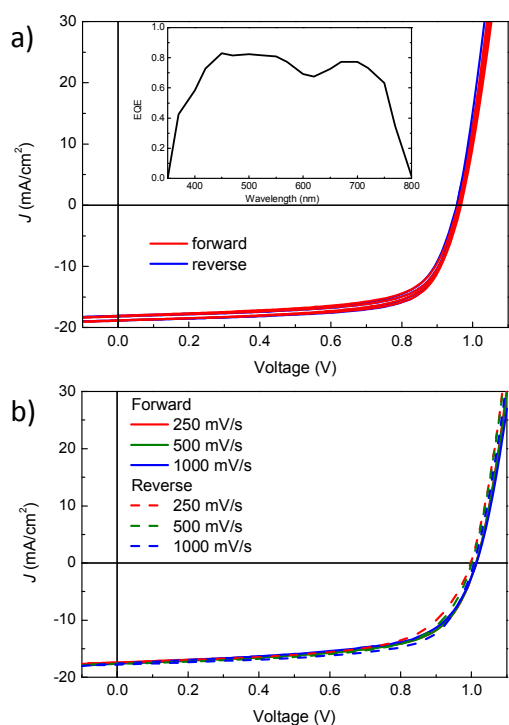


Fig. 3. J-V curves of 4 pixels on the same substrate (a), in forward and reverse scan. The inset shows the EQE of the best performing device. Forward and reverse J-V curves for another set of solar cells measured at different scan rates (b).

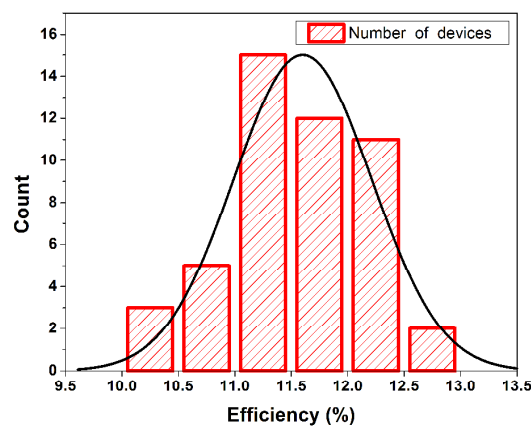


Figure 4. Device efficiency histogram with an overlaid distribution function.

The difference remains rather small, being less than 5% of the measured value for all devices. To further investigate the hysteretic effects, measurements were carried out using different scan speeds (Fig. 3b). We observed very limited hysteresis regardless of the scan rate, with only the FF slightly varying while leaving the V_{oc} and J_{sc} values unchanged. A total of 48 devices were fabricated with this configuration and method. The PCEs recorded at 250 mV/s were ranging from 10.2 % to 12.5 %, which is a fairly narrow distribution, further demonstrating the reproducibility of this approach. Figure 4 shows the histogram of the obtained PCE values with an overlaid normal distribution function. Hence, independent of the scanning speed and direction and consistently over different devices, the J-V characteristics of the solar cells are rather similar, making this approach promising for future optimization and device physics analysis.

Conclusions

We have investigated the effect of an alternative precursor, lead acetate, in the preparation of p-i-n (inverted) perovskite solar cell. The obtained perovskite layers are smooth and pinhole-free over a large area, therefore suitable to be used in combination with thin organic semiconducting transport layers. Solar cells exhibit a remarkably low hysteresis which is also independent on the scan speed. Moreover, the device performances are consistent and stay within a fairly narrow range, indicating the reproducibility of this approach. Finally, the device processing does not involve any high temperature treatment, thus making this approach a good candidate for flexible device fabrication and for the preparation of monolithic tandem perovskite solar cells.

Notes and references

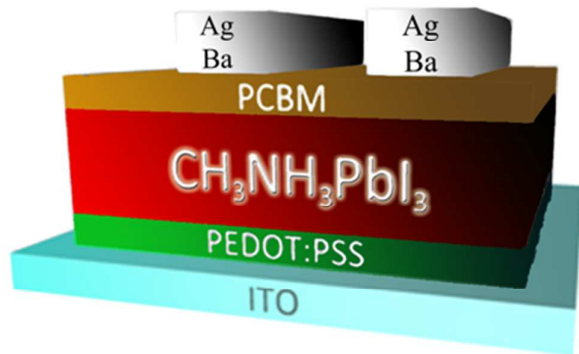
Instituto de Ciencia Molecular, Universidad de Valencia, c/Catedrático J. Beltrán, 2, 46980 Paterna, Spain. E-mail: henk.bolink@uv.es; Fax: +34-963543273; Tel: +34-963544416

Acknowledgements

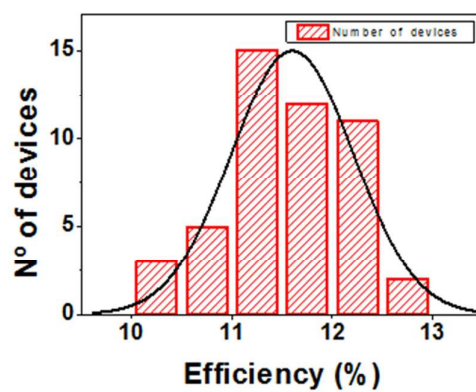
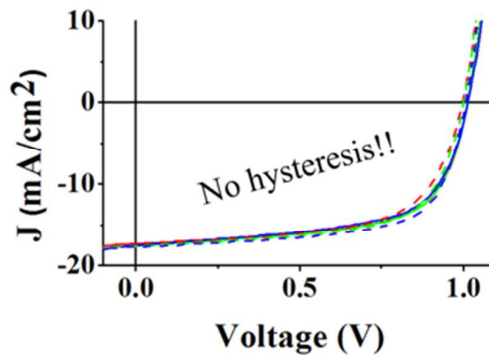
This work has been supported by the the Spanish Ministry of Economy and Competitiveness (MINECO) (MAT2011-24594), and the Generalitat Valenciana (Prometeo/2012/053).

References

1. A. Kojima, K. Teshima, Y. Shirai and T. Miyasaka, *J. Am. Chem. Soc.*, 2009, **131**, 6050-6051.
2. H. S. Jung and N.-G. Park, *Small*, 2015, **11**, 10-25.
3. W.-J. Yin, J.-H. Yang, J. Kang, Y. Yan and S.-H. Wei, 2015, **3**, 8926-8942.
4. D. Shi, V. Adinolfi, R. Comin, M. Yuan, E. Alarousu, A. Buin, Y. Chen, S. Hoogland, A. Rothenberger, K. Katsiev, Y. Losovyj, X. Zhang, P. A. Dowben, O. F. Mohammed, E. H. Sargent and O. M. Bakr, *Science*, 2015, **347**, 519-522.
5. H. J. Snaith, A. Abate, J. M. Ball, G. E. Eperon, T. Leijtens, N. K. Noel, S. D. Stranks, J. T.-W. Wang, K. Wojciechowski and W. Zhang, *J. Phys. Chem. Lett.*, 2014, **5**, 1511-1515.
6. J. a. Christians, J. S. Manser and P. V. Kamat, *J. Phys. Chem. Lett.*, 2015, **6**, 852-857.
7. Y. Tidhar, E. Edri, H. Weissman, D. Zohar, G. Hodes, D. Cahen, B. Rybtchinski and S. Kirmayer, *J. Am. Chem. Soc.*, 2014, **136**, 13249-13256.
8. P.-W. Liang, C.-Y. Liao, C.-C. Chueh, F. Zuo, S. T. Williams, X.-K. Xin, J. Lin and A. K.-Y. Jen, *Adv. Mater.*, 2014, **26**, 3748-3754.
9. Z. Xiao, Q. Dong, C. Bi, Y. Shao, Y. Yuan and J. Huang, *Adv. Mater.*, 2014, **26**, 6503-6509.
10. W. Nie, H. Tsai, R. Asadpour, J.-C. Blancon, A. J. Neukirch, G. Gupta, J. J. Crochet, M. Chhowalla, S. Tretiak, M. a. Alam, H.-L. Wang and A. D. Mohite, *Science*, 2015, **347**, 522-525.
11. A. Buin, P. Pietsch, J. Xu, O. Voznyy, A. H. Ip, R. Comin and E. H. Sargent, *Nano Lett.*, 2014, **14**, 6281-6286.
12. O. Malinkiewicz, A. Yella, Y. H. Lee, G. M. Espallargas, M. Graetzel, M. K. Nazeeruddin and H. J. Bolink, *Nat. Photon.*, 2014, **8**, 128-132.
13. M. Liu, M. B. Johnston and H. J. Snaith, *Nature*, 2013, **501**, 395-398.
14. L. Gil-Escrig, G. Longo, A. Pertegas, C. Roldan-Carmona, A. Soriano, M. Sessolo and H. J. Bolink, *Chem. Commun.*, 2015, **51**, 569-571.
15. C.-w. Chen, H.-w. Kang, S.-y. Hsiao, P.-f. Yang, K.-m. Chiang and H.-w. Lin, *Adv. Mater.*, 2014, **26**, 6647-6652.
16. D. B. Mitzi, M. T. Prikas and K. Chondroudis, *Chem. Mater.*, 1999, **11**, 542-544.
17. F. Wang, H. Yu, H. Xu and N. Zhao, 2015, **25**, 1120-1126.
18. S. a. Kulkarni, T. Baikie, P. P. Boix, N. Yantara, N. Mathews and S. Mhaisalkar, *Journal of Materials Chemistry A*, 2014, **2**, 9221-9225.
19. J.-Y. Jeng, Y.-F. Chiang, M.-H. Lee, S.-R. Peng, T.-F. Guo, P. Chen and T.-C. Wen, *Adv. Mater.*, 2013, **25**, 3727-3732.
20. Y. Wu, A. Islam, X. Yang, C. Qin, J. Liu, K. Zhang, W. Peng and L. Han, *Energy Environ. Sci.*, 2014, **7**, 2934-2938.
21. J. T. Michael M. Lee, Tsutomu Miyasaka, Takuro N. Murakami, Henry J. Snaith, *Science*, 2012, **338**, 643-647.
22. S. Colella, E. Mosconi, P. Fedeli, A. Listorti, F. Orlandi, P. Ferro, T. Besagni, A. Rizzo, G. Calestani, G. Gigli, F. D. Angelis, R. Mosca and F. Gazza, *Chem. Mater.*, 2013, **25**, 4613-4618.
23. D. T. Moore, H. Sai, K. W. Tan, D.-M. Smilgies, W. Zhang, H. J. Snaith, U. Wiesner and L. a. Estroff, *J. Am. Chem. Soc.*, 2015, **137**, 2350-2358.
24. F. M. Yongping Fu , Matthew B. Rowley , Blaise J. Thompson , Melinda J. Shearer , Dewei Ma , Robert J. Hamers , John C. Wright , and Song Jin *J. Am. Chem. Soc.*, 2015, **137**, 5810-5818.
25. L. B. Fadi Kamal Aldibaja, Elena Mas-Marza, Rafael S. Sanchez, Eva M. Barea ´ and a. I. Mora-Sero, *J. Mater. Chem. A*, 2015, **3**, 9194-9200.
26. Y. F. Haiming Zhu, Fei Meng, Xiaoxi Wu, Zizhou Gong, Qi Ding, Martin V. Gustafsson, M. Tuan Trinh, Song Jin & X.-Y. Zhu, *Nat. Mater.*, 2015, **14**, 636-642.
27. W. Zhang, M. Saliba, D. T. Moore, S. Pathak, M. Horantner, T. Stergiopoulos, S. D. Stranks, G. E. Eperon, J. a. Alexander-Webber, A. Abate, A. Sadhanala, S. Yao, Y. Chen, R. H. Friend, L. a. Estroff, U. Wiesner and H. J. Snaith, *Nat. Commun.*, 2014, **6**, 6142.
28. W. Tress, N. Marinova, T. Moehl, S. M. Zakeeruddin, M. K. Nazeeruddin and M. Grätzel, *Energy Environ. Sci.*, 2015, **8**, 995-1004.
29. S. H. Im, J.-H. Heo, H. J. Han, D. Kim and T. Ahn, *Energy Environ. Sci.*, 2015, in press.
30. C.-C. C. Po-Wei Liang, Spencer T. Williams and Alex K.-Y. Jen, *Advanced Energy Materials*, 2015, in press.
31. J. You, Z. Hong, Y. Yang, Q. Chen, M. Cai, T.-B. Song, C.-C. Chen, S. Lu, Y. Liu and H. Zhou, *ACS Nano*, 2014, **8**, 1674-1680.
32. N. J. Jeon, J. H. Noh, W. S. Yang, Y. C. Kim, S. Ryu, J. Seo and S. I. Seok, *Nature*, 2015, **517**, 476-480.



p - i - n



Using a lead acetate precursor p-i-n $\text{CH}_3\text{NH}_3\text{PbI}_3$ perovskite solar cells with remarkable reproducibility and very low hysteresis are reported.